



Research paper

Analysis and field test of transverse force performance of assembled small box girder bridge

Dongyan Zhang¹, Dandan Gu²

Abstract: Continuous assembled box girder bridges are increasingly used in bridge engineering due to their high degree of assembly, short construction period, and high smoothness and comfort of traveling. To grasp the transverse force performance of this type of bridge structure, this paper, based on the industry standard drawings, adopts the method of finite element numerical analysis to systematically study the effects of different miter angles, number of diaphragm girders, span diameters, and width-to-span ratios on the transverse distribution coefficients of the loads and conducts the field test on the real bridge. The results show that the lateral distribution of main girder loads decreases with the increase of miter angle, the increase of the number of diaphragm beams, and the increase of span diameter, and increases with the increase of width-to-span ratio; the field static load tests were carried out on the three bridges, and the measured lateral distribution patterns of the bridge loads match well with the theoretical analysis of the finite element theory. The transverse distribution coefficients of the main girders obtained from the field test are reasonable, indicating that the force distribution of the transverse connection between the main girders is reasonable. The analysis of the transverse force of the assembled small box girder bridge can initially determine whether the bridge integrity is good or not, and provide technical data support for the subsequent operation and maintenance of the bridge.

Keywords: assembled small box girder bridge, transverse force, skew angle, static load test

¹Prof., PhD., College of Computer and Control Engineering, Northeastern Forestry University, No. 26 Hexing Road, Xiangfang District, Harbin City, Heilongjiang Province, China, e-mail: nefuzdhzdy@nefu.edu.cn, ORCID: [0009-0009-5886-6636](https://orcid.org/0009-0009-5886-6636)

²PhD. St., College of Mechanical and Electrical Engineering, Northeastern Forestry University, No. 26 Hexing Road, Xiangfang District, Harbin City, Heilongjiang Province, China, e-mail: gudandan@nefu.edu.cn, ORCID: [0009-0009-0737-6805](https://orcid.org/0009-0009-0737-6805)

1. Introduction

With the rapid development of high-grade highways and urban roads, assembled continuous box girder bridges, which are characterized by saving construction materials, reasonable structural forces, easy quality control, convenient construction, and smooth and comfortable driving, have been widely used [1]. Assembled construction is a fast construction method that combines and assembles the pre-made small box girders at a later stage, so it is necessary to calculate the force of each small box girder in the pre-design and then design, and it is necessary to understand the force of each beam to optimize the construction in the construction stage, as well as to carry out the reasonable operation and maintenance through the force of beam at a later stage, so the force of assembled box girder has gained the attention of the bridge workers. Therefore, the stress condition of the assembled box girder has been paid attention by bridge workers.

Lateral forces in assembled small box girder bridges are affected by various factors. Bridge structure, load location, and vehicle speed are investigated on the troops in continuously assembled multiple box girder bridges [2]. The distribution of transverse live load bending moments of main girders is used to study the forces in straight and curved bridges, and the ratio of span diameter and radius of curvature is obtained to be related to the transverse forces in bridges [3]. Factors such as longitudinal and transverse truck locations, bridge length and width, number of main girders, spacing of main girders, and thickness of slabs are analyzed for their effects on the ultimate capacity of concrete slab-steel girder bridges [4]. The force performance of a single-compartment reinforced concrete skew-curve box girder bridge is investigated and finite elements are modeled to analyze the effects of the parameters skewness and curvature on the force performance of skew-curve box girder bridges [5]. To examine the effect of diagonal crossing on the performance of the bridge under static and dynamic loads, a scaled-down model of a three-span continuous prestressed concrete box girder bridge with a diagonal crossing angle of 45° is tested statically and dynamically [6].

Normally, the load transverse distribution coefficient is used to express the transverse force on the main girder. The load transverse distribution coefficients of multi-girder bridges under specified live loads are investigated [7]. The amount of change in the load transverse distribution coefficient of the calculated girders is utilized to assess the degree of degradation of the transverse force transfer performance of the bridge superstructure [8]. The distribution pattern of eccentric load coefficients of the upper flanges of continuous combined box girder bridges with corrugated steel webs under eccentric loads is used to conclude that it is not appropriate to use uniform eccentric load coefficients for all sections of this bridge type [9]. The transverse load distribution was evaluated by conducting live load tests on bridges in service [10]. A parametric analysis based on 120 bridge information was performed to obtain an improved AASHTO load distribution coefficient calculation formula [7].

Whether the transverse joints of assembled girder bridges are good or not is directly related to the service life of the bridges, which has been studied by some scholars. Hinge joints are crucial parts in assembled multi-girder bridges, and the use of displacement spectrum similarity measure is proposed as an index to assess the critical health of hinges [11]. Static and dynamic load tests on a precast box girder bridge that has been in service for more than 50 years were conducted to study the detection of the presence of damage at the deck slab

joints, and the location of potential deck joint damage can be effectively identified based on the measured changes in the bridge response and model [12]. Deflection is an important parameter in assessing the lateral connections of assembled girder bridges [13, 14].

The method of studying the transverse forces of bridges is mainly a combination of finite element theoretical analysis and real bridge test verification [15–17], and the real bridge load test is an effective means to study the performance of many bridges [18].

There have been fewer studies in the literature on the transverse force performance of assembled small box girder bridges with different skew, this paper takes the industry-standard drawings as the basis and adopts the finite element analysis software to establish the 3D finite element models with different skew angles, different spans, different diaphragm girders and different numbers of beams, to carry out the theoretical analysis of the transverse force of the bridges, and to carry out static loading tests on the example of three real bridges, to carry out the conclusion of the theoretical analysis with the comparison and verification. The research content of this paper has certain guiding significance for the operation, repair, and maintenance of bridges.

2. Orthogonal and Skew bridges

The Orthogonal bridge and Skew bridge are defined in bridge engineering according to the positional relationship between the bridge centerline and the route. Fig. 1 in Shenyang City, Liaoning Province, Xuantu Road, from the west of G1501 Shenyang Roundabout Expressway west 400 m, east to Fushun Wanghua District, along the Bin Road, Xuantu Road, respectively, across two tributaries of the Hun River. From west to east across the first tributary for the location of Bridge 1, across the second tributary for the location of Bridge 2. Observe the position of Bridge 1, the centerline of the route, and the centerline of the main river channel are not perpendicular ($\neq 90^\circ$), but cross together diagonally, and Bridge 1 is a skew bridge at this time. Observe the position of Bridge 2, the centerline of the route and the centerline of the main river channel are perpendicular ($= 90^\circ$), orthogonal relationship, at this time, Bridge 2 is the orthogonal bridge. Based on the route centerline and the bridge centerline is perpendicular to the relationship, divided into the orthogonal bridge and skew bridge, perpendicular relationship that is the orthogonal bridge, and other positional relationships for the skew bridge. When designing Chinese roads, the direction of bridges should obey the linearity of roads, so skew bridges came into being and are widely used in highway bridges and urban bridges.

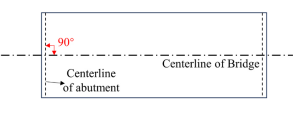
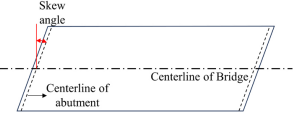
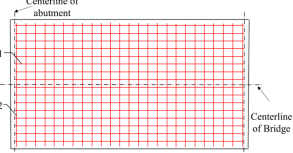
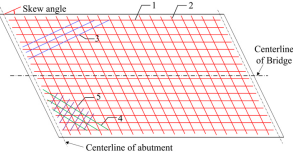
Orthotropic and skew bridges are classified according to the positional relationship between the bridge and the obstacle being crossed (river, road, valley, etc.), which is perpendicular to each other i.e. orthotropic, otherwise diagonal, as shown in Table 1. Because of the existence of skew angles, the geometric shape of the orthotropic bridge in Table 1 is rectangular with all four corners at 90° right angles, and the geometric shape of the skew bridge is a parallelogram with two obtuse and two acute angles. Due to the existence of geometric shape differences, resulting in different force characteristics of the orthotropic and skew bridges, the same span of the orthotropic bridge and the skew bridge for comparison, the orthotropic bridge support reaction is the same, while the skew bridge support reaction in the obtuse angle at the maximum, the acute angle at the minimum, the orthotropic bridge longitudinal bending



Fig. 1. Relationship between bridge and route location

moment is larger than the skew bridge; because of the existence of skew angle, so that the skew bridge in obtuse corners to produce a negative bending moment, which in turn make the skew bridge longitudinal bending moment becomes smaller, while the transverse bending moment increases; When the load is applied to the inclined bridge, the beam deforms differently at the obtuse and acute angles, forming a complex torque.

Table 1. Difference between Orthogonal bridge and Skew bridge

Distinctions		Orthogonal bridge	Skew bridge
Relationship to crossed obstacles		Perpendicular	Oblique
Geometric shape			
Characterization of forces (same span)	Bearing edge reaction force	The same magnitude of the reaction force at the support	Maximum reaction force at two obtuse angles, minimum at acute angles
	Longitudinal bending moment	large	small
	A negative moment at the support point	none	A negative moment at an obtuse angle
	Transverse moment	small	large
	Torsion	none	Complex torque exists
Reinforcing steel construction characteristics			

Due to the different force characteristics of the Orthogonal bridge and Skew bridge, there is a big difference between the two in the construction, according to the force characteristics of the reinforcement arrangement. Orthogonal bridge reinforcement type mainly has No. 1 longitudinal stress steel bar and No. 2 hoop bar, skew bridge based on this reinforcement to increase the perpendicular to the support axis of the No. 3 bar, perpendicular to the obtuse angle bisector of the No. 4 bar and parallel to the obtuse angle bisector of the No. 5 bar, which is completely corresponding to its stress characteristics.

3. Finite element modelling

The finite element analysis model is established by commercial finite element analysis software Midas/Civil, and the model only includes the main components (bridge deck, beams, and bearings). Refer to previous research papers for specific modeling information [19].

In this paper, a total of 50 FEA models are developed to analyse the transverse forces of small box girder bridges using four parameters, namely, skew angle (0° , 15° , 30° , 45°), number of internal diaphragms (0, 1, 3), span diameter (20 m, 25 m, 30 m, 35 m, 40 m), and number of beams (3, 4, 5), as variables.

4. Results and discussion

4.1. Calculation of transverse distribution coefficients

An assembled bridge is a combined structure formed by connecting a beam and a diaphragm beam. When the load moves on the beam, the size of the load borne by each piece of the beam will change, i.e. the force along the beam in the direction of the transverse bridge changes, and the weight of the load borne by each piece of beam is the load transverse distribution coefficient. The transverse load distribution coefficient is used to characterize the size of the transverse force, the larger the coefficient is, the larger the load that the beam is subjected to.

The procedure for calculating the transverse distribution factor of the electrochemical loads for bridges based on the rigid beam method is as follows:

1. According to the finite element model established in Section 3, the deflection of each beam is extracted separately, and the vertical scale of the influence line is found according to Eq. (4.1).

$$(4.1) \quad \eta_{\omega} = \frac{\omega_j}{\sum_{i=1}^n \omega_i}$$

where: η_{ω} – is the vertical scale of the influence line, ω_j – is the deflection of beam j , ω_i – is the deflection of beam i ($i = 1 \sim n$), n – represents the total number of beams.

2. Based on the vertical scale value of the influence line calculated in Step 1, the influence line of the lateral distribution of loads of each beam is plotted.

3. In the lateral distribution of load influence line, the most unfavourable load arrangement is to find the most unfavourable force situation of the bridge when the vehicle moves along the transverse bridge direction, i.e., the influence line of the largest sum of vertical markers is the most unfavourable force situation.
4. Calculation of the lateral load distribution factor.

$$(4.2) \quad m_q = \frac{1}{2}(\eta_{q1} + \eta_{q2} + \eta_{q3} + \eta_{q4} + \cdots + \eta_{qk})$$

where: m_q – is the load lateral distribution coefficient, η_{qk} – represents the impact vertical scale value corresponding to each axle, k – is the number of axles determined according to the number of design lanes, and the design lane is 2, and k is 4.

4.2. Influence of skew angle on transverse forces

Based on the load transverse distribution coefficients calculated in 4.1 for different parameter combinations, the influence of the skew angle on the transverse force performance of the bridge is first analysed. Wanting to explore the degree of influence of the skew angle, the number of internal diaphragm beams and the number of beams are taken as fixed values for analysis. Fig. 2 shows the variation of the load transverse distribution coefficient with a skew angle. Span 30 m, 35 m, 40 m have the same trend, space is limited not to show in detail.

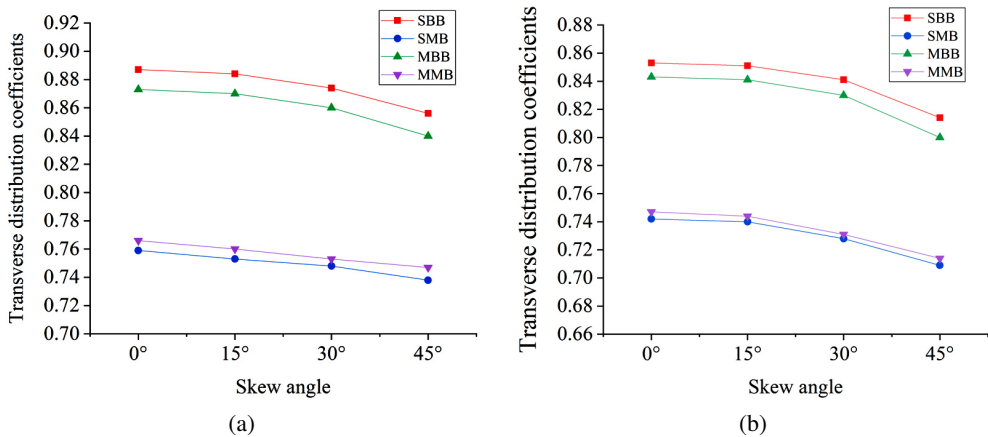


Fig. 2. Variation of load transverse distribution coefficients with skew angle (SBB: Side-span boundary beam; SMB: Side-span middle beam; MBB: Mid-span boundary beam; MMB: Mid-span middle beam); (a) 3×20 m, (b) 3×25 m

As can be seen from Fig. 2, with the increase of the skew angle, the load lateral distribution coefficients of each beam become smaller, and the values of side-span boundary beam and mid-span boundary beams are closer, with a difference of about 0.99%, and the difference between side-span middle beams and mid-span middle beams is about 0.94%. When the skew angle is from 0° to 15°, the change value of the load transverse distribution coefficient is 0.57%,

at this time, the two transverse distribution coefficients are very close to each other, which indicates that the skew angle has less influence on the transverse distribution of the bridge loads, so when the skew angle is less than 15° , it can be calculated according to the design of the orthogonal bridge. When the skew angle changes from 15° to 45° , the curve is steeper, the change rate of the curve from 15° to 30° is 1.95%, and from 30° to 45° is 3.29%, and the increase of the skew angle within the range has a greater effect on the lateral distribution of the loads, which is since as the skew angle increases, the beams is affected by the torsion moment more and more, and the torsion moment increases to reduce the effect of the positive bending moment in the span, which reduces the deflection borne by the beams relatively. The deflection borne by each beam is relatively reduced, showing a decreasing trend. The curves of other spans have the same trend as that of the 20 m span.

4.3. Influence of the number of internal diaphragm beams on transverse forces

To study the effect of the internal diaphragm on the lateral force of the bridge, the same span diameter, skew angle, and width-to-span ratio are set, and the lateral distribution coefficients of the loads are considered when the internal diaphragm is 0, 1, and 3 lanes, respectively.

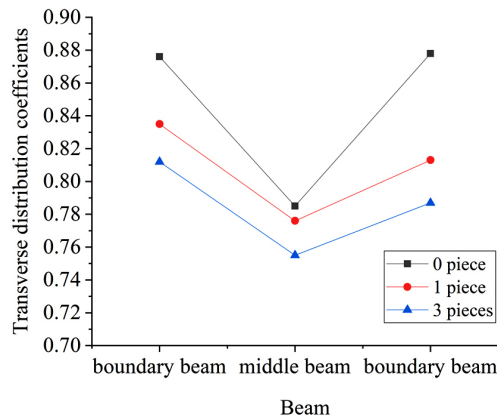


Fig. 3. Variation of load transverse distribution coefficients with the number of internal diaphragm beams

Observing Fig. 3, with the increase of the number of internal transverse beams, the load transverse distribution coefficient gradually becomes smaller, and the difference between the boundary beams and the middle beam becomes smaller, at 0 internal transverse beams, the difference between the boundary beam and the middle beam is 10.49%, the difference between 1 internal transverse beam is 5.82%, and the difference between 3 internal transverse beams is 5.52%, the closer the load transverse distribution coefficients of the boundary beam and the middle beam are, which means that the beams at the various locations are closer to each other in the magnitude of the loads, and the bridge the more uniform the transverse force. Due to the setting of the internal diaphragm, the transverse connection between the beams of the

assembled bridge is more reliable, which improves the bridge integrity, i.e., each beam can better bear the external force together, and the load transverse distribution is more uniform. Increasing the number of diaphragm beams is conducive to improving the integrity, but setting 1 and 3 internal diaphragm beams, the difference in the value of the transverse distribution coefficient is 0.3%, that is, the effect of making the beams uniformly loaded is relatively close to that of the beams, so it is more reasonable to set 1 internal diaphragm beam considering the construction and other factors.

4.4. Influence of span on transverse forces

The relationship between the lateral distribution coefficient and the span diameter is analysed separately for skew angles of 0° , 15° , 30° , and 45° , respectively, and the curves of the load lateral distribution coefficient with the span diameter are shown in Fig. 4. Skew angles of 30° and 45° have the same trend and are not shown in detail for space limitations. Skew angle 15° , 30° have the same trend, space is limited not to show in detail.

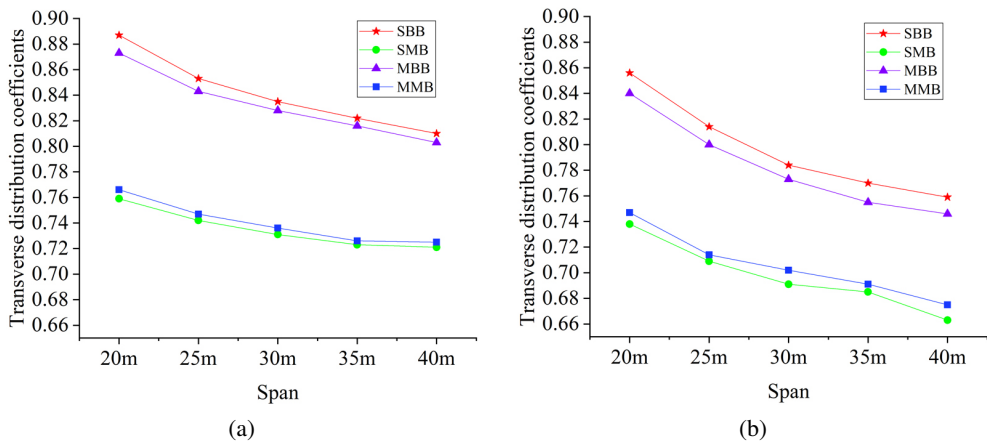


Fig. 4. Variation of load lateral distribution coefficients with span diameter: (a) Skew angle 0° , (b) Skew angle 45°

From the above figure, it can be seen that the lateral load distribution coefficient decreases with the increase of span diameter, and when the skew angle changes from 0° to 45° , the boundary beam decreases by 8.35% to 11.26%, and the middle beam decreases by 5.15% to 9.90%, and the larger the skew angle is, the more obvious the trend of this decrease is. This is because from the structural force analysis, with the increase of span diameter of a continuous beam bridge end negative bending moment also increases, at the same time, a continuous beam bridge due to the increase of end negative bending moment and thus offsets part of the mid-span positive bending moment, the skew angle of the torque also increases gradually, both cases have the effect of reducing the mid-span bending moment.

4.5. Influence of Width-to-span ratio on transverse forces

The ratio of flexural and torsional stiffnesses affects the force characteristics of skew girder bridges in addition to the skew angle of intersection. For box structure, the ratio of flexural and torsional stiffnesses can be expressed in terms of the width-to-span ratio if the bridge span, skew angle, boundary conditions, beam height, and plate thickness remain unchanged. By changing the number of transverse beams to realize the change of the width-to-span ratio, the effect of the width-to-span ratio on the lateral distribution of loads is analysed. In this subsection, the parameter combination of 30° skew angle, 40 m span, and 1 internal diaphragm is selected, and 3 beams, 4 beams, and 5 beams are arranged transversely to realize the variation of the width-to-span ratio.

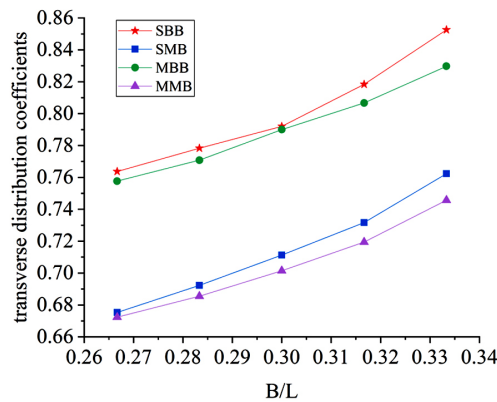


Fig. 5. Variation of load lateral distribution coefficients with aspect ratio

In Fig. 5, the variation of side-span boundary beams and middle beams is 11.63% and 12.89%, respectively, and the variation of mid-span boundary beams and middle beams is 9.51% and 10.91%, respectively, and the coefficient of lateral distribution of the load increases with the increase of the width-to-span ratio but the increase is not significant. The main reason is that the bridge deck becomes wider, the number of beams increases, the number and stiffness of transverse connections remain unchanged, the bridge integralist decreases, and the degree of synergy in which the beams jointly bear the external load decreases, increasing the difference in the load borne by each beam.

5. Field test

In this paper, the static load test is used for the field test, and the structural response of the bridge under load is recorded by loading test, and the observation index is deflection, and then the lateral distribution coefficients of the load deflection of the bridge are obtained, which are compared with the theoretical results of the transverse force of the assembled small box girder bridge in Chapter 4, to verify the transverse force characteristics of the bridge.

5.1. Test bridge background

In this paper, three continuous small box girder bridges are selected for load test, and the information on the three test bridges is shown in Table 2. Bridge 1 and Bridge 3 are compared and analyzed to get the effect of skew angle on the transverse force of the bridge, and the effect of span diameter on the transverse force of the bridge can be obtained by comparing Bridge 2 and Bridge 3.

Table 2. Measured Bridge Parameters

Parameter	Bridge 1	Bridge 2	Bridge 3
Skew (°)	0	30	30
Single span (m)	40	25	40
Number of beams	6	4	4
Bridge width (m)	17.5	12	12
Width-to-span ratio	0.44	0.48	0.30

5.2. Static load test plan

5.2.1. Test sections and measuring points

The static load test of the bridge should be based on the principle of the most unfavorable stress of bridge structure, the principle of representativeness, and the convenience of the test to comprehensively determine the load test bridge span and test section. According to the research purpose of this paper and the provisions of Chinese industry standard JTG/T J21-01-2015, the test section is selected as the mid-span cross-section of the side-span and the middle-span of the continuous girder bridge for the test of deflection.

Figure 6 shows the schematic diagram of the bridge test section, section 1-1 is the center section of the boundary-span bridge, and section 2-2 is the center section of the mid-span bridge. Fig. 6(1-1) is the deflection measurement point layout diagram.

Test conditions

The static load test conditions include the centre load test condition and the eccentric load test condition, as shown in Fig. 7.

Condition 1: Load is distributed at the eccentric position in the cross-section of the side-span (mid-span), and the principle of eccentric arrangement is that the distance between the centre of the outermost wheel and the inner side of the collision wall is 50 cm, and the vehicles are arranged in order, and the distance between neighbouring vehicles is 130 cm, as shown in Fig. 7-condition1.

Condition 2: side-span (middle-span) cross-section of the center of the load distribution, the center of the arrangement of the principle of the center line of the bridge deck as the axis of symmetry symmetrical arrangement of vehicles, the distance between the two vehicles is 130cm, as shown in Fig. 7-condition2.

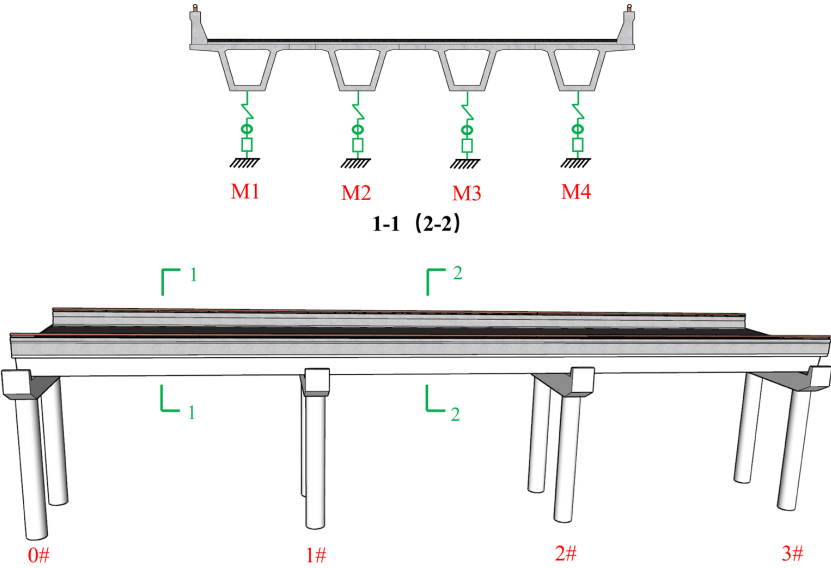


Fig. 6. Test section diagram

Lateral three vehicle layout principles and two vehicles are the same.

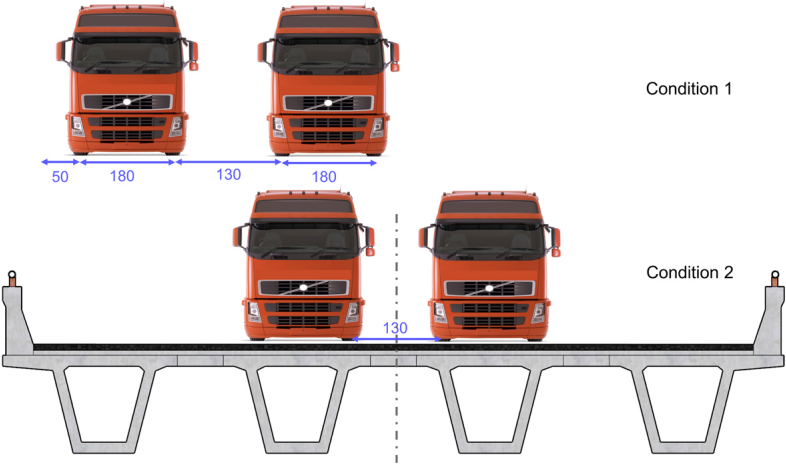


Fig. 7. Schematic diagram of vehicle arrangement for load test condition

Load test vehicle using the test bridge local trucks, according to the prior use of finite element calculation of the number of loaded vehicles and loaded vehicle tonnage for counterweight, the test using the truck type shown in Fig. 8.

The specific test bridges used in the test vehicle parameter information is shown in Table 3.

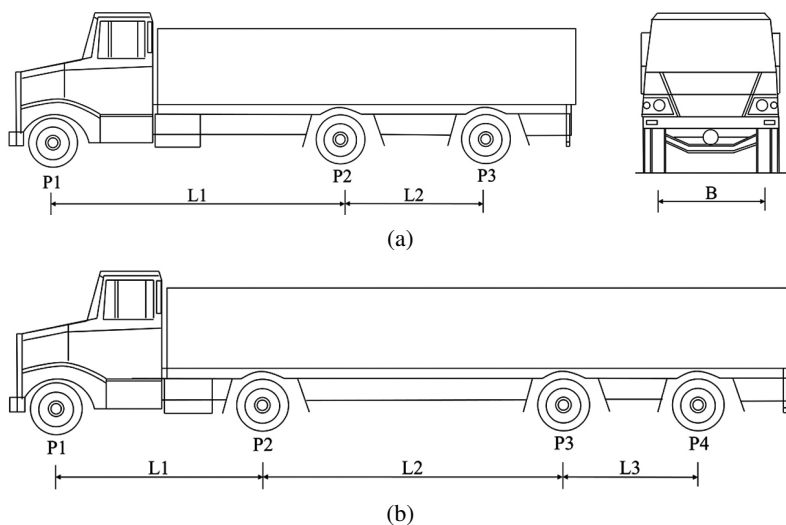


Fig. 8. Test vehicles: (a) 3-axle vehicle, (b) 4-axle vehicle

Table 3. Test vehicle parameter table for each test bridge

Test bridge	Vehicle number	Axle load (t)					Wheelbase and track (m)			
		P1	P2	P3	P4	ΣP	L1	L2	L3	B
Bridge 1	No. 1	10.86	21.71	21.71	—	54.28	3.9	1.4	—	1.8
	No. 2	10.4	20.8	20.8	—	52	3.9	1.4	—	1.8
	No. 3	10.84	21.7	21.7	—	54.24	3.9	1.4	—	1.8
Bridge 2	No. 1	8.92	17.84	17.84	—	44.6	3.5	1.5	—	1.8
	No. 2	9.12	18.24	18.24	—	45.6	3.5	1.5	—	1.8
Bridge 3	No. 1	3.78	8.3	17.78	17.78	47.64	1.8	3.85	1.35	1.8
	No. 2	3.28	8.76	17.69	17.69	47.42	1.8	3.45	1.35	1.8
	No. 3	4.31	8.53	18	18	48.84	1.8	3.45	1.35	1.8

5.2.2. Test process

According to JTG/T J21-01-2015, the testing process of static load test is as follows:

1. The test sequence is first side-span and then the mid-span, from Fig. 8(1-1) to Fig. 8(2-2).

Test vehicle by the bias load test condition 1 into the bridge side-span bridge cross-section, the specific location information see Fig. 9, test vehicle off the engine stationary, while observing the test instrument under the bridge percentile meter pointer, to be the percentile meter pointer stabilized to read the data and record, start the test vehicle forward to carry out the test of the bridge in the mid-span, the same vehicle to reach the designated location, the vehicle off – wait – read and record the data, to complete the condition 1 load test.

2. Carry out the load test in Case 2, location information by Fig. 8 to stop the vehicle, the test sequence is the same as Case 1, the vehicle off – wait – read and record data.
3. Data organization.

5.3. Test Results and Analysis

5.3.1. Influence of skew angle and width-to-span ratio

Bridge 1 and Bridge 3 are two bridges with the same single-span and different skew angles, Condition 1 is the partial load test condition, Condition 2 is the medium load test condition, and the test data of the two conditions are sorted out respectively to obtain the lateral distribution coefficient of load deflection for each condition, as shown in Fig. 9. Middle-span bridge has the same trend, space is limited not to show in detail.

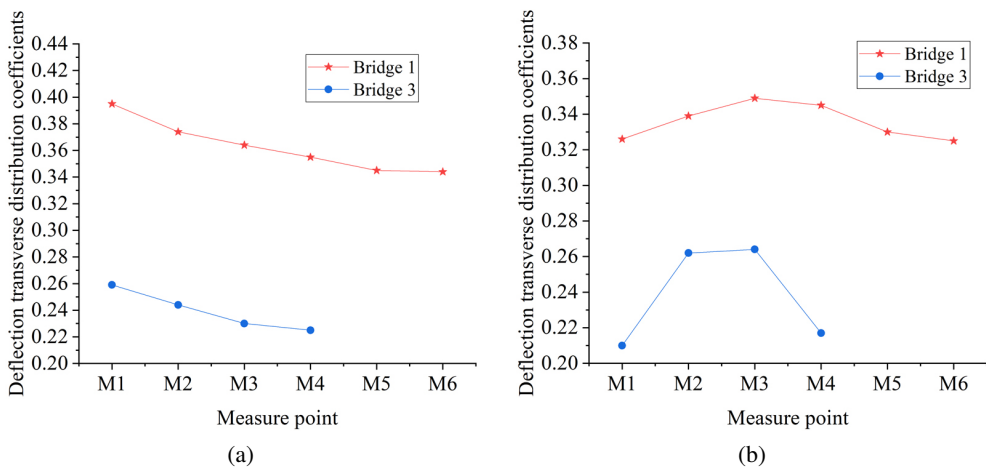


Fig. 9. Lateral distribution coefficients of load deflection for Bridge 1 and Bridge 3 under two working conditions: (a) Side-span bridge (Condition 1), (b) Side-span bridge (Condition 2)

Bridge 1 and Bridge 3 are two bridges with a single span of 40 m. The skew angles are 0° and 30° , respectively. Comparing Bridge 1 and Bridge 3, the deflection transverse distribution coefficients are larger when the skew angle is 30° , and the beams of side spans- have a similar pattern with the beams of mid-span, and the deflection transverse distribution coefficients of bridges with larger skew angles are also larger for centre loading and eccentric loading. Observing the deflection value of each beam, its value is not much different, which indicates that the transverse force of each beam is more uniform, and the integrity of the beam is better.

The B/L of Bridge 1 and Bridge 3 are 0.44 and 0.30, respectively. It can also be observed from Fig. 9 that the lateral distribution coefficient of load deflection of Bridge 1 is larger than that of Bridge 3 for both conditions, which is the same as the law that the lateral distribution coefficient of load increases with the increase of the width-to-span ratio in Section 4.5, which is verified the same way in the real bridge test.

5.3.2. Influence of span

Bridges 2 and 3 are bridges with the same skew angle but different span diameters and the field test results were organized to obtain the static load test data plots of side-span and mid-span bridges under the two conditions, which are shown in Fig. 10. Middle-span bridge has the same trend, space is limited not to show in detail.

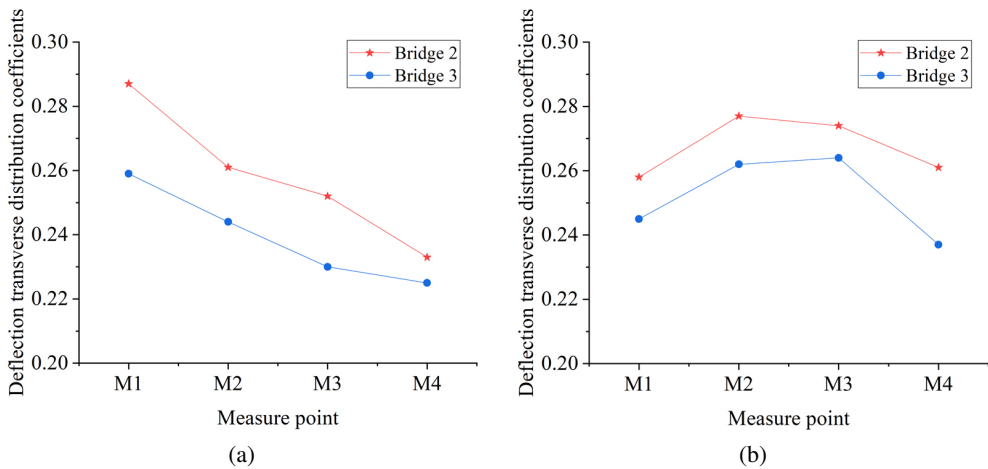


Fig. 10. Lateral distribution coefficients of load deflection for Bridge 2 and Bridge 3 under two working conditions: (a) Side-span bridge (Condition 1), (b) Side-span bridge (Condition 2)

The skew angles of Bridge 2 and Bridge 3 are all 30° , and the single-span are 25 m and 40 m. The lateral distribution coefficients of deflections decrease with the increase of span diameters. The side and middle spans, centre loading, and eccentric loading also have similar stress trends. The difference in deflection values at each beam measurement point is small, indicating that the bridge has good integrity.

Three bridges were tested in the field, and the field test results were consistent with the finite element theoretical analysis. Through the field test results, it is obvious to see the loads borne by each beam. The deflection values of each beam do not show a significant difference, indicating that the transverse force of each beam is more uniform, the connection between the beam is better, and the bridge integrity is better.

6. Conclusions

Assembled continuous small box girder bridges are widely used in engineering with the advantages of reasonable force and a short construction period, etc. Due to the assembled construction method, the transverse force situation of the bridge has received more attention in the design operation and maintenance stages. In this paper, four parameters such as skew angle, number of diaphragm beams, span diameter, and width-to-span ratio are used as variable

parameters to establish a finite element model to systematically analyze the transverse force of the bridge, and the relationship between each parameter and the transverse force of the bridge are obtained. Three representative bridges were tested on-site, and the results of the static load test were consistent with the conclusions obtained from the finite element analysis. The main conclusions can be summarized as follows:

1. The finite element analysis has obtained the relationship between the parameters and the transverse force of the bridge. The skew angle, span diameter, and internal diaphragm beam are negatively correlated with the load transverse distribution coefficient, i.e., the skew angle and span diameter increase the load transverse distribution coefficient to become smaller, but the setting of the internal diaphragm beam needs to be considered comprehensively for the optimization, and the width-to-span ratio is positively correlated with the transverse distribution coefficient. The better the integrity of the bridge, the more uniform the transverse force of the beam.
2. Three representative bridges were tested on-site to verify the relationship between the three parameters of skew angle, span diameter two and width-to-span ratio, and the transverse force of the bridge. The transverse distribution coefficient of the load-deflection obtained from the field test is positively correlated with the skew angle and the span diameter, and negatively correlated with the width-to-span ratio, which is consistent with the conclusion of the finite element analysis, and the effect of the parameter on the transverse force of the bridge is obtained again.
3. By analyzing the transverse force of the bridge, it is necessary to consider the influence of four parameters, namely, skew angle, span diameter, internal diaphragm beam, and width-to-span ratio, when carrying out the design of the bridge, to carry out the design of the small box girder in a targeted way. Through the field test results, the health condition of the bridge in service can be initially assessed, which is of certain significance for the later operation and maintenance of the bridge.

The four parameters of skew angle, span diameter, internal diaphragm beam, and width-to-span ratio have a certain influence on the transverse force of assembled small box girder bridges, but which parameter is more sensitive to the transverse force of bridges is what we need to study in the next step.

References

- [1] Editorial Department of China Journal of Highway and Transport, "Review on China's Bridge Engineering Research:2021", *China Journal of Highway and Transport*, vol. 34, no. 2, pp. 1–97, 2021, doi: [10.19721/j.cnki.1001-7372.2021.02.001](https://doi.org/10.19721/j.cnki.1001-7372.2021.02.001).
- [2] M. Samaan, J.B. Kennedy, and K. Sennah, "Impact Factors for Curved Continuous Composite Multiple-Box Girder Bridges", *Journal of Bridge Engineering*, vol. 12, no. 1, pp. 80–88, 2007, doi: [10.1061/\(ASCE\)1084-0702\(2007\)12:1\(80\)](https://doi.org/10.1061/(ASCE)1084-0702(2007)12:1(80)).
- [3] A.D.S. Rebouças, J.N.D. Silva Filho, R. Barros, Y.R.F. Nascimento, and P.M. Coutinho, "Curved bridges live load bending moment distribution using straight and curved girders", *Revista IBRACON de Estruturas Materiais*, vol. 15, no. 2, p. e15208, 2022, doi: [10.1590/S1983-41952022000200008](https://doi.org/10.1590/S1983-41952022000200008).
- [4] A. Ghani Razaqpur, M. Shedid, and M. Nofal, "Inelastic load distribution in multi-girder composite bridges", *Engineering Structures*, vol. 44, pp. 234–247, 2012, doi: [10.1016/j.engstruct.2012.05.014](https://doi.org/10.1016/j.engstruct.2012.05.014).

- [5] P. Agarwal, P. Pal, and P.K. Mehta, "Parametric study on skew-curved RC box-girder bridges", *Structures*, vol. 28, pp. 380–388, 2020, doi: [10.1016/j.istruc.2020.08.025](https://doi.org/10.1016/j.istruc.2020.08.025).
- [6] X.H. He, X.W. Sheng, A. Scanlon, D.G. Linzell, and X.D. Yu, "Skewed concrete box girder bridge static and dynamic testing and analysis", *Engineering Structures*, vol. 39, pp. 38–49, 2012, doi: [10.1016/j.engstruct.2012.01.016](https://doi.org/10.1016/j.engstruct.2012.01.016).
- [7] S. Kong, L. Zhuang, M. Tao, and J. Fan, "Load distribution factor for moment of composite bridges with multi-box girders", *Engineering Structures*, vol. 215, art. no. 110716, 2020, doi: [10.1016/j.engstruct.2020.110716](https://doi.org/10.1016/j.engstruct.2020.110716).
- [8] S. Wang, J. Du, and H. Su, "Low-Cost Assessment Method for Existing Adjacent Beam Bridges," *Applied Sciences*, vol. 12, no. 21, art. no. 11304, 2022, doi: [10.3390/app122111304](https://doi.org/10.3390/app122111304).
- [9] J. Li, S.S. Law, and H. Hao, "Improved damage identification in bridge structures subject to moving loads: Numerical and experimental studies", *International Journal of Mechanical Sciences*, vol. 74, pp. 99–111, 2013, doi: [10.1016/j.ijmecsci.2013.05.002](https://doi.org/10.1016/j.ijmecsci.2013.05.002).
- [10] S. Hess, F. Filosa, B.E. Ross, and T.E. Cousins, "Live Load Testing of NEXT-D Bridges to Determine Distribution Factors for Moment", *Journal of Performance of Constructed Facilities*, vol. 34, no. 4, art. no. 04020063, 2020, doi: [10.1061/\(ASCE\)CF.1943-5509.0001452](https://doi.org/10.1061/(ASCE)CF.1943-5509.0001452).
- [11] D. Dan, W. Zheng, and Z. Xu, "Research on monitoring index of transverse cooperative working performance of assembled multi-girder bridges based on displacement spectrum similarity measure", *Structures*, vol. 48, pp. 1322–1332, 2023, doi: [10.1016/j.istruc.2023.01.023](https://doi.org/10.1016/j.istruc.2023.01.023).
- [12] M. Abedin, F.J. De Caso y Basalo, N. Kiani, A.B. Mehrabi, and A. Nanni, "Bridge load testing and damage evaluation using model updating method", *Engineering Structures*, vol. 252, art. no. 113648, 2022, doi: [10.1016/j.engstruct.2021.113648](https://doi.org/10.1016/j.engstruct.2021.113648).
- [13] Y. Tian, J. Zhang, Q. Xia, and P. Li, "Flexibility identification and deflection prediction of a three-span concrete box girder bridge using impacting test data", *Engineering Structures*, vol. 146, pp. 158–169, 2017, doi: [10.1016/j.engstruct.2017.05.039](https://doi.org/10.1016/j.engstruct.2017.05.039).
- [14] W. Lu, J. Dong, Y. Pan, G. Li, and J. Guo, "Damage identification of bridge structure model based on empirical mode decomposition algorithm and Autoregressive Integrated Moving Average procedure", *Archives of Civil Engineering*, vol. 68, no. 4, pp. 653–667, 2022, doi: [10.24425/ace.2022.143060](https://doi.org/10.24425/ace.2022.143060).
- [15] S. Alampalli, et al., "Bridge Load Testing: State-of-the-Practice", *Journal of Bridge Engineering*, vol. 26, no. 3, art. no. 03120002, 2021, doi: [10.1061/\(ASCE\)BE.1943-5592.0001678](https://doi.org/10.1061/(ASCE)BE.1943-5592.0001678).
- [16] P. Lu, Z. Xu, Y. Chen, and Y. Zhou, "Prediction method of bridge static load test results based on Kriging model", *Engineering Structures*, vol. 214, art. no. 110641, 2020, doi: [10.1016/j.engstruct.2020.110641](https://doi.org/10.1016/j.engstruct.2020.110641).
- [17] R. Oleszek, W. Radomski, and K. Nowak, "Influence of the type of numerical model a prestressed concrete bridge on the determination of its internal forces and displacements", *Archives of Civil Engineering*, vol. 70, no. 1, pp. 155–167, 2024, doi: [10.24425/ace.2024.148905](https://doi.org/10.24425/ace.2024.148905).
- [18] Z. Zhang, P. Zou, E.-F. Deng, Z. Ye, Y. Tang, and F.-R. Li, "Experimental study on prefabricated composite box girder bridge with corrugated steel webs", *Journal of Constructional Steel Research*, vol. 201, art. no. 107753, 2023, doi: [10.1016/j.jcsr.2022.107753](https://doi.org/10.1016/j.jcsr.2022.107753).
- [19] D. Gu, "Influence of oblique angle on the transverse distribution coefficient of small continuous box girder bridge", *Low Temperature Architecture Technology*, vol. 38 (03), pp. 62–63+75, 2016.

Received: 2024-07-09, Revised: 2024-08-19